

# Two-photon purification of quantum light emission via quantum feedback

Leon Droenner,<sup>\*</sup> Nicolas L. Naumann,<sup>†</sup> Andreas Knorr, and Alexander Carmele  
*Technische Universität Berlin, Institut für Theoretische Physik,  
Nichtlineare Optik und Quantenelektronik, Hardenbergstraße 36, 10623 Berlin, Germany*

A single two-level system acts as a single photon source under a  $\pi$ -pulse excitation. Increasing the pulse area such that the pulse induces a full Rabi-oscillation of the two-level system, a two-photon emission process becomes more probable. We propose a quantum feedback protocol to either choose preferable single or two-photon emission at a  $2\pi$ -pulse excitation. By simulating the feedback reservoir as a matrix-product state within the quantum stochastic Schrödinger picture and by going beyond the common Euler-like expansion, we are able to efficiently deal with light emission in a non-Markovian environment under external time-dependent excitation. Our findings propose quantum interference induced by quantum feedback as an additional control parameter to purify the light emission statistics on demand.

*Introduction.*— Single photons act as qubits for quantum computation protocols [1] or for quantum key distribution [2]. To generate single photons, an almost ideal source is a single two-level system (TLS) [3, 4], realized in e.g. atoms [5], single quantum dots [6–9], molecules [10], and defects in solids [11]. To trigger the emission, one can use a Gaussian pulse in driving a half Rabi-oscillation which inverts the TLS. When decaying radiatively, the TLS spontaneously emits a single photon. Recently it was shown [12–14], that under a pulse which induces a full Rabi-oscillation, the two-photon probability is higher than that for a single photon, providing a single TLS acts as a source for a multi-photon state. For a generation of a two-photon state [15–17], a high degree of control is essential, especially if the same system should act as source for both, single and multi photon generation [18, 19].

In this letter, we propose quantum feedback as an additional control parameter to manipulate the single-photon state via quantum interference of incoming and outgoing fields.

Feedback is used in chaotic systems to stabilize unstable states by specifically exploiting the effect of time-delayed Pyragas control [20–23]. Successful quantum-control protocols use measurement based setups to stabilize non-classical light states [24, 25], cooling of single trapped ions [26] or controlling quantum correlations [27]. Alternatively, one can use structured baths [28] to dissipatively engineer the desired dynamics [29–33]. In these approaches the quantum system is not perturbed by a measurement. The classically successful concept of a finite delay time  $\tau$  for the application of control is transferred to the quantum regime by adding a new aspect to quantum control protocols [34, 35]: The time-delayed signal  $s(t-\tau)$ , for instance induced by back reflection of the signal  $s(t)$  acts as a control parameter, allowing all-optical control while no measurement is needed. By employing feedback in the quantum regime, the entanglement between photons emitted from a biexciton [36] as well as between nodes in a quantum network is controlled [37]. Furthermore, quantum

feedback enhances squeezing in parametric oscillators [38, 39]. In optomechanical systems unstable branches of bistabilities are stabilized using feedback [40]. It was also experimentally demonstrated, that the emission statistics of photonic devices can be manipulated by feedback [41, 42].

In the all-optical quantum feedback, a light reflecting element (mirror, semi-infinite waveguide) feeds back the photons emitted by the system. This way, the surrounding photon reservoir is structured and a non-Markovian treatment is necessary as the emitted photons interact subsequently with the system after a delay time. To overcome this difficulty in the theoretical description, several approaches were proposed in the single excitation regime [43, 44]. Here, we model the feedback with the quantum stochastic Schrödinger equation [45, 46], where a matrix product state (MPS) representation allows to treat only the most relevant part of the Hilbert space corresponding to a numerically exact treatment. In order to deal with the short pulse of the Gaussian shaped excitation, we expand this method by going beyond the Euler-like expansion of the time evolution. This is necessary as two very different timescales, i.e., the short pulse and the long decay, are involved rendering the first order method impractical for this problem. The speedup in the computation also allows a non-Markovian treatment for more complex systems such as strongly-correlated [47–50] or many-emitter setups [51–54].

However, already for a single TLS, our findings clearly demonstrate a quantum interference between the system and the photon-field. These interferences allow the control of the one-photon probability by changing the distance between emitter and mirror. Destructive interference results in a suppression of the one-photon probability and thus increases the chance of a two-photon generation. For constructive interference, a single-photon emission process becomes more probable and the two-photon emission is suppressed resulting in a single-photon source for a  $2\pi$ -pulse. We hereby present a protocol to purify the emission statistics via the distance imposed quantum phase between emitter and mirror.

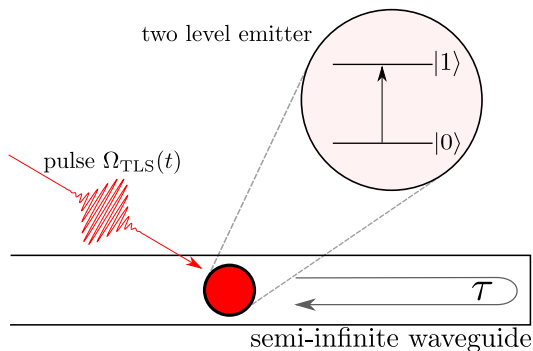


Figure 1. Illustration of the system under pulsed excitation where a single TLS is placed inside a waveguide. Under a Gaussian-shaped pulsed excitation, the system is excited from the ground state  $|0\rangle$  to the excited state  $|1\rangle$  ( $\pi$ -pulse). Due to spontaneous decay, the TLS decays to  $|0\rangle$  and a photon is emitted into the waveguide. A photon propagating to the right side is reflected and may excite the TLS again with delay  $\tau$ . This non-Markovian quantum feedback is essential for the enhancement of the two-photon emission under  $2\pi$ -pulse excitation.

*Model.*— We consider a single TLS inside a semi-infinite waveguide [55, 56], cp. Fig. 1. The TLS is excited via an external coherent pulse, resonant with the TLS-frequency  $\omega_{01}$ . A spontaneous decay of the electronic excited state  $|1\rangle$  emits a photon into the waveguide. The waveguide is closed at the right side, for instance by a reflecting cavity, acting as a mirror. With delay  $\tau$ , the photon again interacts with the TLS. Thus, for a simulation, a memory kernel of the non-Markovian reservoir is needed. For a time discretization of e.g.  $\tau/\Delta t = 100$  and a maximal photon number  $n = 4$  of the reservoir, this would correspond to a Hilbert space of approximate  $3 \times 10^{60}$  states for one  $\tau$ -interval. To efficiently deal with the large Hilbert space, we model it within the quantum stochastic Schrödinger formalism, using MPS [45, 46]. The total Hamiltonian reads  $H_{\text{tot}} = H_{\text{TLS}}(t) + H_{\text{fb}}$ , with

$$H_{\text{TLS}}(t) = \hbar\omega_{01}\sigma_+\sigma_- + \hbar\Omega(t) (\sigma_+e^{-i\omega_L t} + \sigma_-e^{i\omega_L t}) \quad (1)$$

being the Hamiltonian of the pumped two level system in energy conserving rotating wave approximation. The electronic operators are modeled as Pauli-matrices, where  $\sigma_+$  creates and  $\sigma_-$  annihilates an excitation inside the TLS. The external laser is modeled as a Gaussian-pulse with frequency  $\omega_L$  and amplitude

$$\Omega(t) = \frac{A}{\sqrt{\nu^2\pi}} e^{-t^2/\nu^2}, \quad (2)$$

with pulse area  $A$  and the linewidth in terms of the full widths at half maximum  $\nu = \frac{1}{10\Gamma} \frac{1}{\sqrt{2\ln(2)}}$ . We chose the pulse to be short in comparison with the decay of the electronic excited state  $\Gamma$  in the same manner as in Ref.

[13]. For a longer pulse duration, probabilities of higher photon numbers would become more relevant which is beyond the scope of this present study.

The feedback reservoir is modeled as

$$H_{\text{fb}} = \int_{\mathcal{B}} d\omega \hbar\omega b^\dagger(\omega)b(\omega) + \int_{\mathcal{B}} d\omega \hbar [G_{\text{fb}}(\omega)b^\dagger(\omega)\sigma_- + h.c.]. \quad (3)$$

The first term describes the free evolution of the reservoir, with  $b^\dagger(\omega)$  ( $b(\omega)$ ) being the creation (annihilation) operator for a bath photon of frequency  $\omega$ . The TLS-reservoir interaction, is described by  $G_{\text{fb}}(\omega) = g_0 \sin(\omega L/c_0)$  [57–59] with  $c_0$  as the speed of light in vacuum. The coupling  $G_{\text{fb}}(\omega)$  includes the reflecting mirror at distance  $L$  from the TLS with time-delay  $\tau = 2L/c_0$  before an emitted photon again interacts with the TLS. We assume the coupling strengths to be a constant decay parameter  $g_0 = \sqrt{\Gamma}$  of the TLS excitation, which is associated to a Markov approximation. However, the total coupling  $G_{\text{fb}}(\omega)$  includes a sinusoidal dependence on the distance which is a non-Markovian feature induced by the reflecting mirror. Furthermore, we employ the small band approximation, where the relevant system dynamics is assumed to occur in the small bandwidth  $\mathcal{B}$  [46]. By introducing a rotating frame with  $\omega_L$  (assuming resonant excitation  $\omega_L = \omega_{01}$ ) and defining the time-dependent bath operators

$$b(t) = \frac{1}{\sqrt{2\pi}} \int_{\mathcal{B}} d\omega b(\omega) e^{-i(\omega - \omega_L)t} \quad (4)$$

the Hamiltonian is written as

$$H_{\text{TLS,rf}}(t) = \hbar\Omega(t) (\sigma_+ + \sigma_-), \quad (5)$$

$$H_{\text{fb,rf}} = -i\hbar \left( \sqrt{\frac{\Gamma}{2}} b(t - \tau) e^{-i\phi} + \sqrt{\frac{\Gamma}{2}} b(t) \right) \sigma_{10} + h.c.. \quad (6)$$

We define the feedback phase  $\phi = \pi - \omega_{01}\tau$  resulting in constructive ( $\omega_{01}\tau = 2n\pi$ ) or destructive interference ( $\omega_{01}\tau = (2n - 1)\pi$ ) of the TLS with the feedback photon field.

*Numerical evaluation.*— The dynamics are governed by the time evolution operator

$$U(t_{k+1}, t_k) = \hat{T} \left[ \exp \left( -\frac{i}{\hbar} \int_{t_k}^{t_{k+1}} dt' H(t') \right) \right]. \quad (7)$$

We discretize the time by applying  $U(t_{k+1}, t_k)$  on the state  $|\Psi(t_k)\rangle$  with time step  $\Delta t = t_{k+1} - t_k$ . Note that  $|\Psi(t_k)\rangle$  has a large relevant Hilbert space including the system and the non-Markovian reservoir which is why we solve it via the MPS formalism. Applying  $U(t_{k+1}, t_k)$  on  $|\Psi(t_k)\rangle$ , correlations between system and reservoir are induced. We use a singular-value decomposition (SVD) for

$|\Psi(t_{k+1})\rangle$  in order to express it again as an MPS and get rid of the large Hilbert space problem by neglecting the zero singular values.

Due to the short pulsed excitation  $\Omega(t)$  compared to the TLS decay  $\Gamma$ , two different time scales are involved. A small  $\Delta t$  is crucial to govern the exact dynamics during the short pulse. We go beyond the common Euler-like expansion of  $U(t_{k+1}, t_k)$  [46] by expanding the time-evolution to a higher order. This makes an efficient simulation of the time-dependent excitation possible by choosing a higher  $\Delta t$  and thus reducing the number of SVDs. Furthermore, we calculate correlation functions of photon operators up to the third order to disentangle them in order to derive the photon distribution up to three photons. Thus, three integrals over all time steps have to be evaluated. By choosing a higher  $\Delta t$  due to the higher order in  $U(t_{k+1}, t_k)$ , we drastically reduce the total number of time steps with the same accuracy and the calculation of correlation functions speeds up significantly. We explain the higher order in  $U(t_{k+1}, t_k)$  and the algorithm using MPS more detailed in the appendix.

The photon statistics have to be evaluated directly from the bath modes. To calculate the photon probabilities from the reservoir correlation functions we use the relation between correlation functions and photon probabilities. For a single photon mode, the  $m$ th order intensity correlation function is computed from the photon probability [12] by

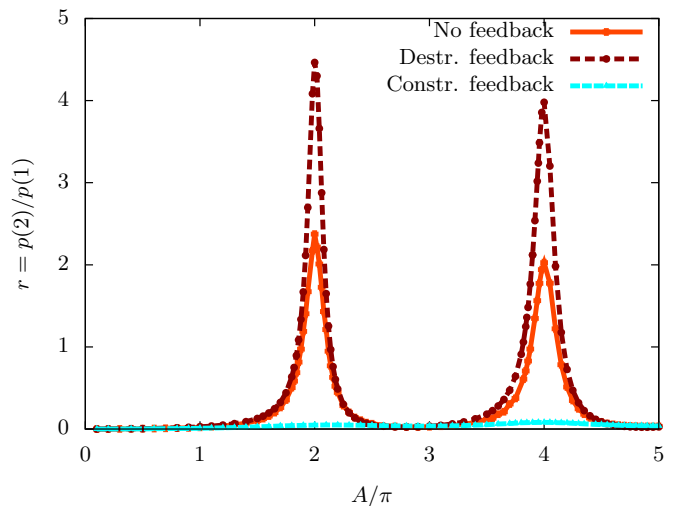
$$C_m = \langle : \hat{I}^m : \rangle = \sum_{n=0}^{\infty} \frac{n!}{(n-m)!} p(n), \quad (8)$$

where  $C_1 = \int_0^\infty dt \langle b^\dagger(t)b(t) \rangle$  represents the photon intensity. We expand this up to  $C_3$  which is the third order correlation function. Since the Hamiltonian does not include a multiphoton generation process (e.g.  $b^\dagger b^\dagger$ ), the reason for  $p(2) > p(1)$  is a multiple single photon generation due to multiple spontaneous decay during the driving pulse  $\Omega(t)$ . This allows us to assume any correlations higher than third order to be negligible as either  $p(1)$  or  $p(2)$  is dominant and  $p(3)$  is comparably small for all investigated pulses and vanishes if the pulse duration is lowered sufficiently. We explain the numerical expensive calculation of the non-local (in time) correlation functions from the MPS more detailed in the appendix. The correlation functions, experimentally accessible via an integrated measurement of the unnormalized autocorrelation functions  $\int_0^\infty dt_1 \dots \int_0^\infty dt_m G^{(m)}(t_1, \dots, t_m)$ , give access to the photon probabilities of interest. Cutting the expansion in Eq. (8) after the third order, the photon probabilities read:

$$p(1) = C_1 - C_2 + \frac{C_3}{2}, \quad (9a)$$

$$p(2) = \frac{C_2 - C_3}{2}, \quad (9b)$$

$$p(3) = C_3/6. \quad (9c)$$



(a) No feedback (b) Destructive (c) Constructive

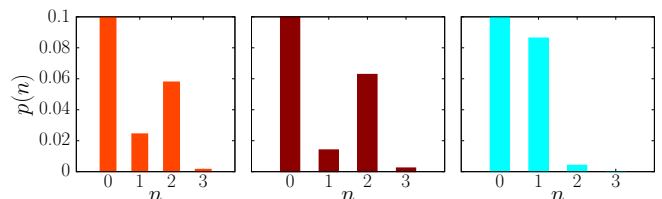


Figure 2. Top: Two-photon dominance  $r = p(2)/p(1)$  versus the pulse area of the excitation pulse  $A$ . Without feedback (solid, orange), at  $A = 2n\pi$  ( $n \geq 1$ ), the two-photon generation dominates over single photon emission  $r > 1$ . Applying feedback with destructive interference ( $\phi = 0$ , dashed red), the ratio is nearly doubled at  $A = 2n\pi$ . Bottom: Photon probabilities  $p(n)$  at  $A = 2\pi$ . (a) Benchmark with Ref. [13] for the case without feedback. (b) Applying destructive feedback ( $\tau\Gamma = 0.11$ ),  $p(1)$  decreases drastically and  $p(2)$  slightly increases. In contrast, for constructive feedback ( $\phi = 1$ , (c)) it is vice versa and a single photon dominates over two-photon emission. The feedback mechanism enhances the two-photon emission via quantum interference. The additional feedback control parameter (mirror distance) allows to chose either a one- or a two-photon emission process at the same excitation pulse.

With our method we are able to obtain the same probabilities as in Ref. [13], where a single TLS, excited with a  $2\pi$ -pulse, shows  $p(2) > p(1)$ . This was obtained via quantum trajectories and experimentally verified. We include quantum feedback with the mirror distance as an additional control parameter and show a nearly doubled ratio  $r = p(2)/p(1)$  for two-photon emission.

*Controlled enhancement or suppression of the one- to two-photon probability ratio*— Over a wide range of the area  $A$  of the externally applied pulse, a single photon emission is the dominant process. First, we discuss the case without feedback, cp. Fig. 2 (top, orange solid line), which shows the ratio  $r = p(2)/p(1)$ . For  $r \rightarrow 0$ , single photon emission dominates. This is especially the case

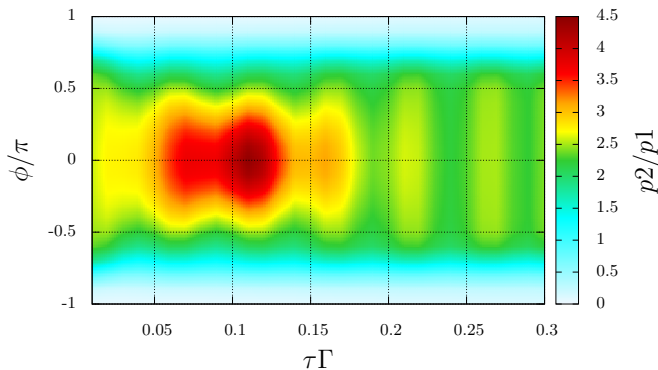


Figure 3. Feedback-phase dependency of the ratio  $p(2)/p(1)$ . Both probabilities show clearly a sinusoidal dependence on the feedback phase  $\phi$ . While a single photon is most probable for constructive feedback with the TLS ( $\phi = \pi$ ), the two-photon probability is maximal for destructive feedback ( $\phi = 0$ ) and even higher than in a setup without feedback. Furthermore,  $p(1)$  is suppressed for destructive interference. Varying  $\tau$ , an interference pattern becomes visible with areas where  $p(1)$  is suppressed stronger (red/yellow areas)

for a pulse area  $A = \pi$  of the coherent excitation. However, at  $A = 2\pi$ , where the excitation pulse induces a full Rabi-oscillation of the TLS, the two-photon probability  $p(2)$  is higher than  $p(1)$  with  $r > 1$ . The TLS changes from a single photon source to a two photon emitter. This counter intuitive behavior was already shown for the case without feedback and explained with a quantum trajectory simulation [13, 14]. During the excitation pulse, the TLS might decay and emit a photon. The remaining pulse re-excites the TLS and a second photon is emitted on a long timescale  $1/\Gamma$ . This can be directly observed in the photon distribution  $p(n)$ , cp. Fig. 2(bottom, (a)). Next, including a properly designed controllable feedback mechanism, introducing destructive interference of the photon field with the TLS (cp. text after eq. (6)), the ratio  $r = p(2)/p(1)$  is nearly doubled at  $A = 2n\pi$  (Fig. 2 top, dashed red). This is due to single-photon suppression (Fig. 2 bottom, (b)). The probability  $p(1)$  is suppressed at the simultaneous increase of  $p(0)$  but also  $p(2)$  and  $p(3)$  are increased slightly. If the feedback is constructive (Fig. 2 bottom, (c)), the effect is reversed. In this case,  $p(1)$  is the dominant probability compared to  $p(2)$  and  $p(3)$  which are suppressed. Thus, a change of the feedback phase allows to either enhance or suppress the single-photon probability. For a  $2\pi$ -pulse, where  $p(2) > p(1)$ , it either enhances or eliminates the effect of a dominant two-photon emission.

To explain this effect of the feedback in more detail, we show the feedback phase dependency of the ratio  $r$  in Fig. 3 for  $A = 2\pi$ . The feedback phase depends on both,  $\phi$  and  $\tau$ . For clarity, we split the fast  $\phi$  and the slow oscillations  $\tau$  (cp. Eq. (6)), both are accessible by varying the mirror distance  $L$ . The  $p(1)$  as well as the  $p(2)$  probability show a sinusoidal dependence by

varying  $\phi$ . While  $p(1)$  is maximal for  $\phi = \pi$ , for  $p(2)$  it is vice versa at  $\phi = 0$ , where  $p(1)$  is minimal. Thus, the ratio  $r$  is always maximal at  $\phi = 0$  and minimal at  $\phi = \pi$ . By varying  $\tau$ , we always observe  $p(1) > p(2)$  at  $\phi = \pi$  ( $r \rightarrow 0$ ). For destructive interference ( $\phi \approx 0$ ), we find a clear two-photon enhancement compared with the case without feedback at  $\tau\Gamma \approx 0.11$ . For other delay-times  $\tau$  we observe smaller ratios  $r$ . However, the feedback protocol always shows the same or higher ratio  $r$  compared to the case without feedback around  $\phi = 0$ . We highlight, that by varying  $\tau$  the ratio  $r$  alternates which we refer to interference patterns. Note, that  $p(3)$  is two orders of magnitudes smaller than  $p(2)$  and has the same phase dependency (on both,  $\phi$  and  $\tau$ ) as  $p(2)$  which is due to the multiple photon creation during the pulse.

If  $\phi = \pi$ , the photon-field interferes constructively with the TLS, thus effectively resulting in a smaller decay  $\Gamma$ . This makes a two-photon excitation during the pulse less probable. As a consequence, the photon number decreases and shows a single photon statistic. This is reversed for destructive interference  $\phi = 0$ , which effectively results in a higher radiative decay than without feedback. Due to the effective higher decay, a two-photon emission during the pulse is more probable, which is why  $p(2)/p(1)$  increases compared to a setup without feedback. We stress that still a zero-photon emission process is the most probable. By increasing the pulse duration compared to  $\Gamma$ ,  $p(2)$  increases but also higher photon probabilities than  $p(3)$  become relevant.

*Conclusion.*— Our findings prove a quantum interference effect between the photon-field and the TLS, resulting in a higher chance of two-photon emission compared to the case without feedback. By adding an additional control parameter, which is time delay due to a feedback geometry, we predict a controllable setup for choosing either an enhancement of the two-photon emission process or a single photon process at pulse area  $A = 2\pi$ , by varying the feedback/mirror distance.

We thank Florian Katsch for helpful discussions. The authors gratefully acknowledge the support of the Deutsche Forschungsgemeinschaft (DFG) through the project B1 of the SFB 910 and by the School of Nanophotonics (SFB 787).

## Appendix

In order to simulate quantum feedback in an efficient way, we use the quantum stochastic Schrödinger equation [46]. By writing the state of the system and the reservoir in a matrix product state, one can cut the zero value Schmidt coefficients and thus efficiently deal with a large Hilbert space. Initially, the system is in the state  $|\Psi(0)\rangle$ . We discretize the time  $\Delta t = t_{k+1} - t_k$  and the state

at a specific time bin is written as  $|\Psi(t_k)\rangle$ . By applying the discrete time evolution operator  $U(t_{k+1}, t_k)$ , the state evolves in time to the next time step  $|\Psi(t_{k+1})\rangle$  with

$$U(t_{k+1}, t_k) = \hat{T} \left[ \exp \left( -\frac{i}{\hbar} \int_{t_k}^{t_{k+1}} dt' H(t') \right) \right]. \quad (\text{A.10})$$

For arbitrary  $t_k$  and  $t_{k+1}$ , the time ordering  $\hat{T}$  has to be respected. However, if the Hamiltonian commutes with itself at different times  $[H(t), H(t')] = 0$ ,  $t \neq t'$  [60], the time ordering is obsolete. In the Hamiltonian used in the manuscript, the only operators that do not commute at different times are  $b(t)$  and  $b^\dagger(t' - \tau)$ , when  $t = t' - \tau$ . If we restrict the time step to  $\Delta t < \tau$ , this case will not occur in the above integration. Thus, the integration can be evaluated in the exponential without the time ordering operator in Eq. (A.10) allowing us to define the photon bin operators  $\Delta B(t_k) = \int_{t_k}^{t_{k+1}} dt b(t)$ . These operators obey the commutation relations

$$[\Delta B(t_j), \Delta B^\dagger(t_k)] = \Delta t \delta_{j,k}. \quad (\text{A.11})$$

We introduce the basis states

$$|i_p\rangle = \frac{(\Delta B^\dagger(t_p))^{i_p}}{\sqrt{i_p! \Delta t^{i_p}}} |\text{vac}\rangle. \quad (\text{A.12})$$

in the same manner as in Ref. [46]. In addition, we expand the time evolution operator to a higher order, in order to deal with the two different time scales of the pulsed excitation scheme.

### Higher order time evolution

We expand the time evolution operator to a higher order in  $\Delta t$  by computing a matrix exponential. Here, we explain it with the Hamiltonian of the main manuscript. To write the Hamiltonian in matrix form, we use the basis  $|i_S, i_n, i_\tau\rangle$ , where  $i_S$  is the level of the TLS,  $i_n$  is the occupation of the photon bin at the current time step  $t_k$  and  $i_\tau$  is the occupation of the photon bin at time step  $t_{k-l} = t_k - \tau$ . With this, we get the system matrix  $\mathbf{M}_{\text{TLS,env}}(t_n)$  with the matrix elements

$$\begin{aligned} & -\frac{i}{\hbar} \langle j_S, j_n, j_\tau | \int_{t_k}^{t_{k+1}} H_{\text{TLS}}(t) dt | i_S, i_n, i_\tau \rangle \\ &= -i \Delta t [\Delta_{01} \delta_{j_S,1} \delta_{i_S,1} \\ & \quad + \Omega(t_n) (\delta_{j_S,1} \delta_{i_S,0} + \delta_{j_S,0} \delta_{i_S,1})] \delta_{i_S,1} \delta_{j_n, i_n} \delta_{j_\tau, i_\tau}. \end{aligned}$$

We assumed the enveloping function  $\Omega(t)$  to be slowly varying in the time step  $\Delta t$ . Furthermore, we used that the system operators are not explicitly time-dependent. The feedback reservoir matrix we write with the above

defined operators as

$$\begin{aligned} \int_{t_k}^{t_{k+1}} H_{\text{fb}} dt &= -i \hbar \left( \sqrt{\frac{\Gamma}{2}} \Delta B(t_{k-l}) e^{-i\phi} \right. \\ & \quad \left. + \sqrt{\frac{\Gamma}{2}} \Delta B(t_k) \right) (\sigma_{10} + \sigma_{21}) + h.c. \end{aligned} \quad (\text{A.13})$$

This results in the matrix elements for the feedback matrix  $\mathbf{M}_{\text{fb}}$

$$\begin{aligned} & -\frac{i}{\hbar} \langle j_S, j_n, j_\tau | \int_{t_k}^{t_{k+1}} H_{\text{fb}} dt | i_S, i_n, i_\tau \rangle \\ &= -\left( \sqrt{\frac{\Gamma}{2}} \sqrt{i_\tau} \delta_{j_\tau+1, i_\tau} e^{-i\phi} + \sqrt{\frac{\Gamma}{2}} \sqrt{i_n} \delta_{j_n+1, i_n} \right) \\ & \quad \times \delta_{j_S,1} \delta_{i_S,0} \sqrt{\Delta t} \\ & \quad + \left( \sqrt{\frac{\Gamma}{2}} \sqrt{i_\tau} \delta_{j_\tau+1, i_\tau} e^{-i\phi} + \sqrt{\frac{\Gamma}{2}} \sqrt{i_n} \delta_{j_n+1, i_n} \right) \\ & \quad \times \delta_{j_S,1} \delta_{i_S,0} \sqrt{\Delta t}. \end{aligned}$$

Note, that the matrix  $\mathbf{M}_{\text{TLS,env}}(t_n) \propto \Delta t$ , while  $\mathbf{M}_{\text{fb}} \propto \sqrt{\Delta t}$ .

We extract the time dependency of the pulsed excitation in order to deal with time independent matrices of the system, defining the matrix  $\mathbf{M}_{\text{TLS}} = \mathbf{M}_{\text{TLS,env}}(t_n) / \Omega(t_n)$ . This has computational reasons as only the enveloping function  $\Omega(t)$  changes with each time step. When evaluating the evolution matrix in higher order, all terms of  $\Delta t$  up to the desired order have to be taken into account in the expansion

$$\begin{aligned} \mathbf{U} &= \exp(\Omega(t_n) \mathbf{M}_{\text{TLS}} + \mathbf{M}_{\text{fb}}) \\ &= \sum_{p=0}^{\infty} \frac{1}{p!} (\Omega(t_n) \mathbf{M}_{\text{TLS}} + \mathbf{M}_{\text{fb}})^p. \end{aligned} \quad (\text{A.14})$$

For the first order evaluation in  $\Delta t$ , as used in [46], terms up to the order  $p = 2$  in the expansion of  $\mathbf{U}$  contribute, as  $\mathbf{M}_{\text{fb}} \propto \sqrt{\Delta t}$ . Thus, for second order expansion in  $\Delta t$  terms up to  $p = 4$  in Eq. (A.14) have to be considered. We use the expansion to second order which reads explicitly

$$\begin{aligned} \mathbf{U} &\approx \mathbf{U}_0 + \Omega(t) \mathbf{U}_1 + \Omega(t)^2 \mathbf{U}_2 \\ &= \mathbb{1} + \mathbf{M}_{\text{fb}} + \frac{1}{2} \mathbf{M}_{\text{fb}}^2 + \frac{1}{6} \mathbf{M}_{\text{fb}}^3 + \frac{1}{24} \mathbf{M}_{\text{fb}}^4 \\ & \quad + \Omega(t_n) \left[ \mathbf{M}_{\text{TLS}} + \frac{1}{2} (\mathbf{M}_{\text{TLS}} \mathbf{M}_{\text{fb}} + \mathbf{M}_{\text{fb}} \mathbf{M}_{\text{TLS}}) \right. \\ & \quad \left. + \frac{1}{6} (\mathbf{M}_{\text{TLS}} \mathbf{M}_{\text{fb}}^2 + \mathbf{M}_{\text{fb}} \mathbf{M}_{\text{TLS}} \mathbf{M}_{\text{fb}} + \mathbf{M}_{\text{fb}}^2 \mathbf{M}_{\text{TLS}}) \right] \\ & \quad + \Omega(t_n)^2 \frac{1}{2} \mathbf{M}_{\text{TLS}}^2. \end{aligned}$$

The second line is the time-independent part of the evolution matrix  $\mathbf{U}_0$ , in the third and fourth line the

time-dependence enters linearly and gives the linear part  $\Omega(t_n)\mathbf{U}_1$ . The last line is quadratic in the pump and gives the part  $\Omega(t_n)^2\mathbf{U}_2$ . With this, the time evolution matrices of each order can be computed from the matrices  $\mathbf{M}_{\text{fb}}$  and  $\mathbf{M}_{\text{TLS}}$  by simple matrix multiplications. The enveloping function only needs to be evaluated once each time step. The time evolution of the system is evaluated by the sum

$$|\Psi(t_{k+1})\rangle = [\mathbf{U}_0 + \Omega(t)\mathbf{U}_1 + \Omega(t)^2\mathbf{U}_2] |\Psi(t_k)\rangle. \quad (\text{A.15})$$

This can be simplified by saving the matrices  $\mathbf{U}_i$  as sparse matrices so that the matrix multiplications are only marginally slower than for the time-independent evolution.

The following procedure is the same as in Ref. [46]. The state of the total system is written as a matrix product state by assuming that the bath is initially in a vacuum state. The subsequent application of  $\mathbf{U}$  will introduce correlations between system and bath. The state  $|\Psi\rangle = \sum_{\{i\}} \psi_{\dots, i_k, i_S, \dots, i_{k-l}, \dots, i_k, i_S, i_{k-1}, \dots, i_{k-l}, \dots}$  is represented as a matrix product state with the coefficients

$$\psi(t_k)\{i\} = A_{i_k, \alpha_k}^{[k]} A_{\alpha_k, i_S, \beta_S}^{[S]} A_{\beta_S, i_{k-1}, \beta_{k-1}}^{[k-1]} \dots A_{\beta_{-l}, i_{-l}}^{[-l]}. \quad (\text{A.16})$$

The tensors  $A$  represent either photon bins or the system. These tensors already include the singular values. We use this representation in order to avoid numerical issues due to the multiplication with the inverse of small singular values. In this representation, the single  $A$ -tensor which currently is left- as well as right-normalized has to be kept track of, as it needs to be included if any operation is performed.

In order to apply the time evolution with the long range interaction involving  $t_k$  and the possibly distant  $t_{k-l}$  the photon bin at  $t_{k-l}$  is brought next to the system bin by performing swap operations. However, each time

step  $2(l-1)$  swap operations need to be performed and each swap requires a SVD. The greatest advantage in using a higher order in  $U(t_{k+1}, t_k)$  is the higher possible step size  $\Delta t = t_{k+1} - t_k$  with the same accuracy of the result. Thus in total, less steps need to be performed. In addition, a single step needs fewer SVDs as  $l = \tau/\Delta t$  becomes smaller and results in a high speedup of the computation. A disadvantage of the higher order in  $\mathbf{U}$  is that multi-photon processes become possible in a single time step. Thus, additional photon states in the bath modes have to be taken into account. However, this additional complexity is outweighed by far by the speedup due to the reduction in SVDs.

### Computation of the reservoir correlations

To compute the correlation functions, we define the operator for the total intensity emitted into the environment as  $\hat{I} = \sum_{j=-\infty}^{\infty} \Delta B^\dagger(t_j)\Delta B(t_j)$ . This is the total intensity inside the bath modes. For the numerical evaluation, we note, that there will be no light emitted into the environment before time  $t = -\tau = -q\Delta t$ , as we assume an initial vacuum state and after a large enough time  $t_{\text{end}} = N\Delta t$ , all excitation from the TLS will be emitted into the bath, so that afterwards no photons will be observed. The  $m$ th order intensity correlation function will be given by  $\langle : \hat{I}^m : \rangle$ , where  $:$  indicates the normal ordering of the operators. We relate this to the total probability of  $n$  photons  $p(n)$  which results in

$$C_m = \langle : \hat{I}^m : \rangle = \sum_{n=0}^{\infty} \frac{n!}{(n-m)!} p_{\text{tot}}(n). \quad (\text{A.17})$$

As argued in the main text, we will consider the photon probability up to third order. This becomes explicitly

$$C_1 = \sum_{k=-q}^N \langle \Delta B^\dagger(t_k)\Delta B(t_k) \rangle \quad (\text{A.18a})$$

$$C_2 = \sum_{k=-q}^N \sum_{l=-q}^N \langle \Delta B^\dagger(t_k)\Delta B^\dagger(t_l)\Delta B(t_l)\Delta B(t_k) \rangle \quad (\text{A.18b})$$

$$C_3 = \sum_{k=-q}^N \sum_{l=-q}^N \sum_{m=-q}^N \langle \Delta B^\dagger(t_k)\Delta B^\dagger(t_l)\Delta B^\dagger(t_m)\Delta B(t_m)\Delta B(t_l)\Delta B(t_k) \rangle. \quad (\text{A.18c})$$

These photon correlations are computed from the MPS that was evolved to time  $t_{\text{end}}$ . As the above correlation functions are non-local expectation values in time, their

computation becomes numerically expensive for large time differences. In order to obtain the total correlation, we need to sum over all times. The computation of



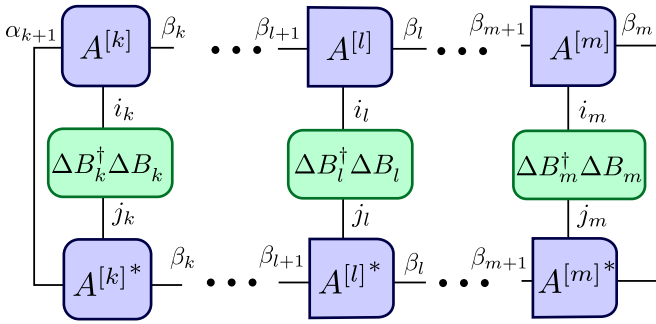


Figure 4. Computation of the third order correlation function Eq. A.18c from the MPS in diagrammatic form. For each time combination, the intensity operator is applied at the corresponding time steps. The cost of this operators grows linearly with the difference  $|k - m|$ .

these correlations from the MPS is exemplary shown in Fig. 4 in diagrammatic form. According to the commutation relation in Eq. (A.11), the correlations are invariant under the reordering of the bath operators at different times. We can use this symmetry to reduce the cost of the numerical evaluation.

\* droenner@itp.tu-berlin.de; These two authors contributed equally

† These two authors contributed equally

- [1] J. L. O'Brien, *Science* **318**, 1567 (2007).
- [2] T. Jennewein, C. Simon, G. Weihs, H. Weinfurter, and A. Zeilinger, *Phys. Rev. Lett.* **84**, 4729 (2000).
- [3] M. O. Scully and S. Zubairy, *Quantum Optics* (Cambridge University Press, 2008).
- [4] M. Kira and S. W. Koch, *Semiconductor quantum optics* (Cambridge University Press, 2011).
- [5] B. Darquié, M. P. A. Jones, J. Dingjan, J. Beugnon, S. Bergamini, Y. Sortais, G. Messin, A. Browaeys, and P. Grangier, *Science* **309**, 454 (2005).
- [6] A. J. Shields, *Nat Photon* **1**, 215223 (2007).
- [7] V. A. Gaisler, *Bulletin of the Russian Academy of Sciences: Physics* **73**, 77 (2009).
- [8] S. Buckley, K. Rivoire, and J. Vučković, *Reports on Progress in Physics* **75**, 126503 (2012).
- [9] Heinze Dirk, Breddermann Dominik, Zrenner Artur, and Schumacher Stefan, *Nature Communications* **6**, 8473 (2015).
- [10] B. Lounis and W. E. Moerner, *Nature* **407**, 491 (2000).
- [11] I. Aharonovich, D. Englund, and M. Toth, *Nat Photon* **10**, 631641 (2016).
- [12] J. Lindkvist and G. Johansson, *New Journal of Physics* **16**, 055018 (2014).
- [13] K. A. Fischer, L. Hanschke, J. Wierzbowski, T. Simmet, C. Dory, J. J. Finley, J. Vuckovic, and K. Muller, *Nature Physics* **13**, 649 (2017).
- [14] K. A. Fischer, L. Hanschke, J. J. Finley, K. Müller, and J. Vučković, *arXiv preprint arXiv:1708.05444* (2017).
- [15] E. del Valle, S. Zippilli, F. P. Laussy, A. Gonzalez-Tudela, G. Morigi, and C. Tejedor, *Phys. Rev. B* **81**, 035302 (2010).
- [16] E. del Valle, A. GonzalezTudela, E. Cancellieri, F. P. Laussy, and C. Tejedor, *New Journal of Physics* **13**, 113014 (2011).
- [17] P. R. Sharapova, K. H. Luo, H. Herrmann, M. Reichelt, C. Silberhorn, and T. Meier, *Phys. Rev. A* **96**, 043857 (2017).
- [18] L. Schneebeli, M. Kira, and S. W. Koch, *Phys. Rev. Lett.* **101**, 097401 (2008).
- [19] Jahnke Frank, Gies Christopher, Aßmann Marc, Bayer Manfred, Leymann H. A. M., Foerster Alexander, Wiersig Jan, Schneider Christian, Kamp Martin, and Höfling Sven, *Nature Communications* **7**, 11540 (2016).
- [20] K. Pyragas, *Phys. Rev. E* **66**, 026207 (2002).
- [21] E. Schöll and H. G. Schuster, *Handbook of Chaos Control* (Wiley-VCH, 2008).
- [22] E. Schöll, S. H. Klapp, and P. Hövel, *Control of self-organizing nonlinear systems* (Springer, 2016).
- [23] R. Lang and K. Kobayashi, *IEEE J. Quantum Electron.* **16**, 347 (1980).
- [24] C. Sayrin, I. Dotsenko, X. Zhou, B. Peaudecerf, T. Rybarczyk, S. Gleyzes, P. Rouchon, M. Mirrahimi, H. Amini, M. Brune, J.-M. Raimond, and S. Haroche, *Nature* **477**, 73 (2011).
- [25] H. Wiseman and G. Milburn, *Quantum Measurement and Control* (Cambridge University Press, Oxford, 2006).
- [26] P. Bushev, D. Rotter, A. Wilson, F. m. c. Dubin, C. Becher, J. Eschner, R. Blatt, V. Steixner, P. Rabl, and P. Zoller, *Phys. Rev. Lett.* **96**, 043003 (2006).
- [27] V. Sudhir, D. J. Wilson, R. Schilling, H. Schütz, S. A. Fedorov, A. H. Ghadimi, A. Nunnenkamp, and T. J. Kippenberg, *Phys. Rev. X* **7**, 011001 (2017).
- [28] J. F. Poyatos, J. I. Cirac, and P. Zoller, *Phys. Rev. Lett.* **77**, 4728 (1996).
- [29] H.-P. Breuer, E.-M. Laine, J. Piilo, and B. Vacchini, *Rev. Mod. Phys.* **88**, 021002 (2016).
- [30] W. T. Strunz, L. Diósi, and N. Gisin, *Phys. Rev. Lett.* **82**, 1801 (1999).
- [31] Á. Rivas, S. F. Huelga, and M. B. Plenio, *Reports on Progress in Physics* **77**, 094001 (2014).
- [32] A. Metelmann and A. A. Clerk, *Phys. Rev. X* **5**, 021025 (2015).
- [33] D. O. Krimer, B. Hartl, and S. Rotter, *Phys. Rev. Lett.* **115**, 033601 (2015).
- [34] C. U. Lei and W.-M. Zhang, *Annals of Physics* **327**, 1408 (2012).
- [35] A. L. Grimsmo, *Phys. Rev. Lett.* **115**, 060402 (2015).
- [36] S. M. Hein, F. Schulze, A. Carmele, and A. Knorr, *Phys. Rev. Lett.* **113**, 027401 (2014).
- [37] S. M. Hein, F. Schulze, A. Carmele, and A. Knorr, *Phys. Rev. A* **91**, 052321 (2015).
- [38] M. Kraft, S. M. Hein, J. Lehnert, E. Schöll, S. Hughes, and A. Knorr, *Phys. Rev. A* **94**, 023806 (2016).
- [39] N. Német and S. Parkins, *Phys. Rev. A* **94**, 023809 (2016).
- [40] N. L. Naumann, S. M. Hein, A. Knorr, and J. Kabuss, *Phys. Rev. A* **90**, 043835 (2014).
- [41] F. Albert, C. Hopfmann, S. Reitzenstein, C. Schneider, S. Hfling, L. Worschech, M. Kamp, W. Kinzel, A. Forchel, and I. Kanter, *Nature Communications* **2**, 366 (2011).
- [42] C. Hopfmann, F. Albert, C. Schneider, S. Hfling, M. Kamp, A. Forchel, I. Kanter, and S. Reitzenstein,

- New Journal of Physics **15**, 025030 (2013).
- [43] A. Carmele, J. Kabuss, F. Schulze, S. Reitzenstein, and A. Knorr, Phys. Rev. Lett. **110**, 013601 (2013).
- [44] J. Kabuss, D. O. Krimer, S. Rotter, K. Stannigel, A. Knorr, and A. Carmele, Phys. Rev. A **92**, 053801 (2015).
- [45] C. Schön, E. Solano, F. Verstraete, J. I. Cirac, and M. M. Wolf, Phys. Rev. Lett. **95**, 110503 (2005).
- [46] H. Pichler and P. Zoller, Phys. Rev. Lett. **116**, 093601 (2016).
- [47] R. Nandkishore and D. A. Huse, Annu. Rev. Condens. Matter Phys. **6**, 15 (2015).
- [48] M. Žnidarič, A. Scardicchio, and V. K. Varma, Phys. Rev. Lett. **117**, 040601 (2016).
- [49] E. Levi, M. Heyl, I. Lesanovsky, and J. P. Garrahan, Phys. Rev. Lett. **116**, 237203 (2016).
- [50] L. Droenner and A. Carmele, Phys. Rev. B **96**, 184421 (2017).
- [51] D. Wigger, T. Czerniuk, D. E. Reiter, M. Bayer, and T. Kuhn, New Journal of Physics **19**, 073001 (2017).
- [52] T. Czerniuk, D. Wigger, A. V. Akimov, C. Schneider, M. Kamp, S. Höfling, D. R. Yakovlev, T. Kuhn, D. E. Reiter, and M. Bayer, Phys. Rev. Lett. **118**, 133901 (2017).
- [53] N. L. Naumann, L. Droenner, W. W. Chow, J. Kabuss, and A. Carmele, J. Opt. Soc. Am. B **33**, 1492 (2016).
- [54] L. Droenner, N. L. Naumann, J. Kabuss, and A. Carmele, Phys. Rev. A **96**, 043805 (2017).
- [55] S. Hughes, Phys. Rev. Lett. **98**, 083603 (2007).
- [56] Y.-L. L. Fang and H. U. Baranger, Phys. Rev. A **91**, 053845 (2015).
- [57] U. Dorner and P. Zoller, Phys. Rev. A **66**, 023816 (2002).
- [58] N. Trautmann and G. Alber, Phys. Rev. A **93**, 053807 (2016).
- [59] F. M. Faulstich, M. Kraft, and A. Carmele, Journal of Modern Optics **0**, 1 (2017).
- [60] W. P. Schleich, *Quantum Optics in Phase Space* (Wiley-VCH, 2001).